Eur Radiol (2011) 21:2103–2110
DOI 10.1007/s00330-011-2146-y

CARDIAC

Multidetector CT imaging of mechanical prosthetic heart valves: quantification of artifacts with a pulsatile in-vitro model

Petr Symersky · Ricardo P. J. Budde · Paul Westers · Bas A. J. M. de Mol · Mathias Prokop

Received: 2 March 2011 / Revised: 15 April 2011 / Accepted: 27 April 2011 / Published online: 15 May 2011

Abstract
Objectives Multidetector computed tomography (MDCT) can detect the cause of prosthetic heart valve (PHV) dysfunction but is hampered by valve-induced artifacts. We quantified artifacts of four PHV using a pulsatile in-vitro model and assessed the relation to leaflet motion and valve design.
Methods A Medtronic Hall tilting disc (MH), and Carbomedics (CM), St Jude (SJM), and ON-X bileaflet valves underwent CT in an in-vitro model using retrospective gating with a 64 detector CT system in stationary and pulsatile conditions. Artifacts and radiopaque component volumes were quantified with thresholds based on surrounding structures and valvular components.
Results Hypodense artifacts volumes (mm^3) were 1,029±147, 535±53, 371±16, and 366±18 for the SJM, MH, CM and ON-X valves ($p<0.001$ except for the latter two valves $p=0.43$). Hyperdense artifact volumes were 3,546±141, 2,387±103, 2,003±102, and 3,033±31 for the SJM, MH, CM and ON-X valve, respectively (all differences $p<0.001$). Leaflet motion affected hypodense ($F=41.5$, $p<0.001$) and hyperdense artifacts ($F=53.7$, $p<0.001$). Closed and moving leaflets were associated with the least and the most artifacts respectively ($p<0.001$, both artifact types).
Conclusion Both valve design and leaflet motion affect PHV-induced artifacts. Best imaging results may be expected for the CM valve during phases in which the leaflets are closed.

Keywords Heart valve prosthesis · CT · Artifacts · In-vitro · Cardiac

P. Symersky (✉)
Department of Cardiothoracic Surgery,
Onze Lieve Vrouwe Gasthuis,
Oosterpark 9, P.O box 95500, 1090 HM, Amsterdam,
The Netherlands
e-mail: psymersky@gmail.com

P. Symersky · B. A. J. M. de Mol
Department of Cardiothoracic Surgery, Academic Medical Center,
Amsterdam, The Netherlands

R. P. J. Budde
Department of Radiology, University Medical Center,
Utrecht, The Netherlands

P. Westers
Department of Biostatistics,
Julius Center for Health Sciences and Primary Care,
Utrecht, The Netherlands

B. A. J. M. de Mol
Department of Biomedical Engineering,
University of Technology Eindhoven,
Eindhoven, The Netherlands

M. Prokop
Department of Radiology,
Radboud University Nijmegen Medical Center,
Nijmegen, The Netherlands

Introduction

Metal implants are an important cause of artifacts on CT imaging. Artifacts may preclude diagnostic evaluation of structures adjacent to metallic implants such as the distal ureter in the case of hip prosthesis and cerebrovascular structures in the case of neurosurgical clips [1–4]. Implant-related artifacts depend not only on size but also on the

constituent metal. For example, CT angiography after the use of titanium clips yields remarkably better image quality than clips made of a cobalt alloy [4]

Recently, CT imaging has been explored as a new imaging modality for mechanical prosthetic heart valves (PHV) [5–8]. Conventionally, PHV function is monitored by echo-Doppler. Leaflet motion can be assessed with fluoroscopy due to the manufacturers' addition of tungsten to the leaflets. Both of these techniques have limitations: acoustic shadowing precludes imaging of periprosthetic anatomy with echo-Doppler and fluoroscopy shows leaflet motion only. The cause of dysfunction, such as interference with subprosthetic tissue, may require reoperation for the replacement of the dysfunctional prosthetic valve. However, the surgical findings may differ significantly from preoperative diagnosis and in some cases no abnormalities can be found [9, 10]. Initial experience with CT has shown that CT can detect morphological abnormalities that explain abnormally high transprosthetic Doppler velocities [5, 7, 8]. In fact, CT may help differentiate between various causes of obstruction and thereby help to determine the need for surgery [7].

Due to their function, PHV are a unique category of implants. Contrary to most other metal implants which are largely static, PHV inevitably exhibit two forms of motion: 1) motion of the valve as a whole due to the motion of the heart and 2) motion of the leaflets. Currently used PHV are relatively similar with respect to their components: all have a metal prosthetic ring and all have tungsten-impregnated carbon leaflets. Despite these common components, important differences exist in the periprosthetic image quality when tested in vitro [11] and when scored clinically [12]. These disparities have been tentatively attributed to the differences in configuration of these hyperdense components but, to our knowledge, no detailed study has been undertaken to quantify prosthesis-related artifacts in MDCT imaging of PHV. This study has the goal to quantify and compare artifacts generated by four commonly used PHV in a pulsatile in-vitro model and determine how valve design and leaflet motion affect artifacts.

Methods

In vitro model

An in-vitro model was used that was described in detail earlier [11]. In short, it consisted of a pump-driven mock loop that connected to a custom-made polymethyl methacrylate (PMMA) valve chamber. The valve chamber had a central mounting ring (under a 45° angle to the CT gantry) in which various valve prostheses could be mounted and was placed in the central circular space of a commercially available anthropomorphic thoracic phantom (QRM GmbH, Möhrendorf, Germany). An ECG signal synchronized to the aortic flow pulse generator was generated by the software for ECG-gated image acquisition. For this study, the in-vitro model was set to produce flow pulses with the ejection phase lasting 50% of the total pulsation cycle at a frequency of 60 per minute.

Valve prostheses

Four currently used mechanical valve aortic prostheses were examined (Fig. 1): St Jude masters bileaflet (SJM, St Jude Medical Inc., St Paul MN), Medtronic Hall tilting disc (MH, Medtronic Inc., Minneapolis MN), Carbomedics aortic reduced bileaflet (CM, Carbomedics Inc., Austin TX), ON-X bileaflet (ON-X Life Technologies Inc., Austin, TX). We chose the same nominal diameter of 27 mm for all valves. Valve leaflets consisted of carbon impregnated with 5 or 10% tungsten and coated with a pyrolytic carbon coating. The valve housing consisted of the prosthetic ring which held the pivot mechanism for the leaflets and a rotation mechanism for the suture cuff. The MH valve had a prominent central titanium strut and a titanium hinge

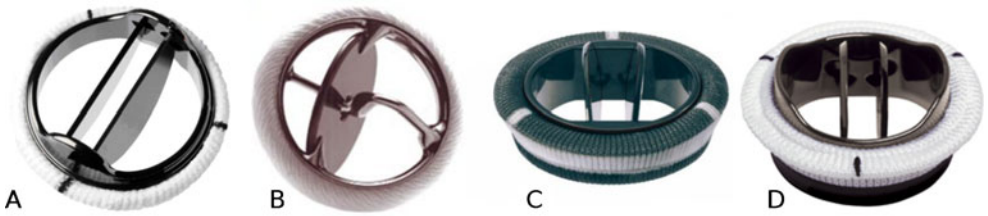

Fig. 1 The four types of mechanical aortic valves used. The St Jude (**a**) and the Medtronic Hall (**b**) valve are pictured from below and the Carbomedics (**c**) and ON-X (**d**) valve are pictured from above. Note the variable position of the leaflet hinge points. The hinge points are below the level of the housing ring in the St Jude valve (**a**) and are at the level of the housing ring in the Carbomedics (**c**) and ON-X (**d**) valves. The Medtronic Hall valve (**b**) is the only tilting disc valve and has a housing ring and central struts made of titanium. The elongated housing ring of the ON-X valve contains two titanium rings. (Images courtesy of St Jude Medical Inc., St Paul MN, Medtronic Inc., Minneapolis MN, Carbomedics Inc., Austin TX, ON-X Life Technologies Inc., Austin, TX)

mechanism. Valves were tightly mounted in the PMMA valve chamber ensuring complete fixation during the pump cycle and eliminating potential artifacts generated by movement of the valve as a whole. The MH tilting disc valve was mounted with the largest orifice superiorly. The bileaflet valves were orientated with the leaflets opening vertically.

Image acquisition

Imaging was performed using 64 multidetector CT (Brilliance 64, Philips Medical Systems, Best, the Netherlands). Data were acquired using retrospective ECG gating and a 64× 0.25 mm collimation, a pitch of 0.2, a gantry rotation time of 420 ms at 120 kVp and 600 mAs. ECG-gated data sets were reconstructed retrospectively at each 10% of the R-R interval from the raw data and transferred to a dedicated workstation for analysis.

Measurement protocol

For each valve, 20 CT data acquisitions were performed with a stationary closed valve to obtain baseline artifact volumes for each specific valve type. These images were reconstructed using commercially available analysis software (Philips Brilliance 3.0, Philips Medical Systems, Best, the Netherlands). The CT densities of the prosthetic ring, the valve leaflets, fluid (water) and surrounding PMMA structure were measured 20-fold. The threshold value for hypodense artifacts was established by using HU value of the least dense periprosthetic structure (water, 4±18 HU) and subtracting 3 times the SD. The threshold for hyperdense artifacts was derived from the CT density of the surrounding PMMA structure (130±23 HU) and adding 3 times the SD. The latter threshold included not only the volume affected by artifacts but also the volume of the hyperdense valve components (ring and leaflets).

For differentiation of leaflet and metal components, threshold values were derived from the least dense leaflet and ring compounds, respectively, and subtracting approximately 3 times the SD. A corrected hyperdense artifact volume was determined by subtracting the volume of the hyperdense valve components (ring and leaflets) from the volume above the 200 HU threshold.

Unrelated sources of artifacts (such as lung volumes of the phantom) were digitally "excised". All artifact volumes were calculated on a CT workstation (Extended Brilliance Workstation, Philips Medical Systems, Best, the Netherlands) from the volume of the voxels within the valve chamber that were within the defined threshold ranges.

For pulsatile valves, seven CT examinations were performed per valve. Each CT data acquisition generated 10 data image sets (at every 10% of the R-R interval). Using the 3D volumetric thresholds described above, the artifact volume was measured in the volume rendered images for each reconstruction phase. Thus, for each valve 70 measurements were done for the hyperdense and for the hypodense artifacts. For every measurement, the position of the valve leaflets was noted as either closed, opening, opened or closing. For visualization purposes, volume rendered images were created that rendered those image regions transparent that were outside the relevant density range.

To test the relation between leaflet motion and artifact volume, four R-R intervals were identified which corresponded to the four phases of leaflet motion: 1) closed, 2) opening, 3) opened, 4) closing. In addition, the artifact volumes of the closed stationary valves were compared to the pulsatile valves with closed leaflets.

Statistics

Measurements were compared using ANOVA with posthoc Bonferroni testing for parametrically distributed data. For nonparametric data a Kruskall Wallis test and a post hoc Mann Whitney *U* test was used for testing between valves.

For the pulsatile valves, a repeated measures analysis for each threshold was performed using ECG reconstruction interval as within factor and valve type as between factor. Posthoc Bonferroni tests were used to compare between intervals and valve types. For the four phases of leaflet motion a repeated measures analysis was done with four ECG intervals as within factor and valve type as between factor. Statistical calculations were performed using commercially available software (SPSS 16.0, Chicago, IL). Statistical significance was defined as $p<0.05$.

Results

The densities of the prosthetic ring and leaflets varied between valves. The SJM had the highest prosthetic ring density (3,035±19 HU) although the difference with the MH (2,986±24 HU) and CM (2,976±26 HU) valves was small. The ON-X valve ring was considerably less dense (2,202±64 HU). For the leaflets the densities of the MH and CM (1,767±147 and 1,791±203, respectively) valve were higher than the SJM and ON-X leaflets (1,410±131 and 1,402±201, respectively). The threshold for the leaflets and ring were derived from the lowest leaflet and ring densities (of the ON-X valve) and subtracting 3SD resulting in thresholds of 800 and 2,000 for the leaflets and ring respectively.

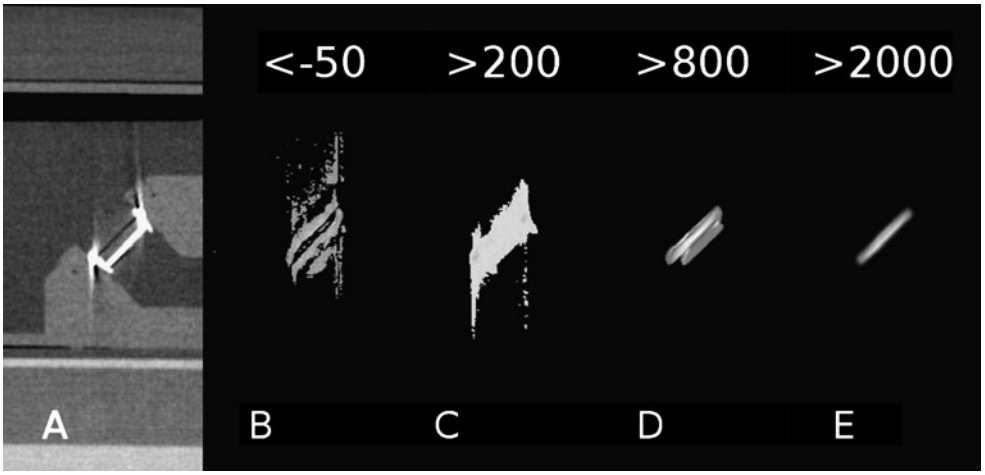

Fig. 2 A Sagittal view of a St Jude valve prosthesis on multiplanar reformatting (**a**). The valve is placed in the mounting ring of the valve chamber which is inserted in the thoracic phantom at a 45° angle to the CT gantry. Volume rendered images of the same valve with the −50 (**b**) and 200 (**c**) threshold. The 800 threshold (**d**) includes prosthetic ring and leaflets and the 2,000 threshold (**e**) includes only the prosthetic ring

The different thresholds demonstrated various configurations of artifacts (Fig. 2). Specific testing between pairs of static valves indicated differences between all valves for the 2,000, 800 and 200 HU thresholds (Table 1, $p<0.001$). For the −50 HU threshold no difference was found between the ON-X and CM valves ($p=0.43$) but all other differences were significant ($p<0.001$). The differentiation of the volume attributable to radiopaque components of the valve such as the ring and the leaflets from the total 200 HU threshold volume is demonstrated in Fig. 3. Specific testing between specific components demonstrated significant differences between ring volumes: 480±3, 745±12, 611±12 and 147±3 mm^3 for the SJM, MH, CM and ON-X valve respectively (all differences $p<0.001$). The leaflet volumes were 975±11, 1,111±25, 1,101±15, and 1,336±8 mm^3 for the SJM, MH, CM and ON-X valve respectively. No difference existed between the CM and MH valve ($p=0.33$), but the SJM and the ON-X had respectively a smaller and a larger leaflet volume than the other valves ($p<0.001$). The artifact volumes (without leaflet and ring components) were 3,546±141 mm^3 for the SJM, 2,387±103 mm^3 for the MH, 2,003±102 mm^3 for the CM, and 3,033±31 mm^3 for the ON-X valve (all differences $p<0.001$).

For pulsatile valves, leaflet motion was present during the 10% and 20% ECG intervals (leaflet opening motion in 100% and 49% of the valves respectively) and during the 60% and 70% ECG intervals (closing motion in 86% and 49% of the valves respectively). Leaflets were completely opened in all valves at 30–50% of the ECG interval and completely closed during 80–90 and 0% of the ECG interval (see Fig. 4).

Analysis of pulsatile valves demonstrated a strong effect of the interval on hypodense ($F=41.5$, $p<0.001$) and hyperdense artifacts ($F=53.7$, $p<0.001$). The interpolation lines in the graphical depictions of the pulsatile artifacts (Fig. 5) follow a similar and mostly parallel pattern. There was no relevant interaction with valve type ($F=6.3$ and 7.0, for hypo- and hyperdense artifacts respectively).

Four ECG intervals were identified which corresponded to the 4 phases of leaflet motion: 0% closed, 10% opening, 40% opened, 60% closing. Comparison of the 4 intervals for hypo- and hyperdense artifacts yielded the least artifacts for closed leaflets (both $p<0.001$) followed by opened ($p=0.046$ and $p<0.001$ for hypo- and hyperdense artifacts respectively). The largest artifact volumes were found for either opening or closing leaflets ($p<0.001$ for both artifact types, no difference between opening and closing). Post hoc analysis revealed higher increase of both types of artifacts for the MH valve compared to the other valves.

Pulsatile valves with closed leaflets exhibited more hypodense artifacts than stationary valves with closed leaflets ($p<0.001$ all valves). The average increases for pulsatile valves were 52%, 25%, 42% and 44% for the ON-X, SJM, CM and MH valve respectively. For the hyperdense artifacts, only the ON-X valve displayed a relative increase for the pulsatile closed valves ($p<0.001$). No

Table 1 Volumes (mm^3) measured with the different thresholds

Valve type	<−50	> 200	>800	>2,000
St Jude	1,029±147	5,001±143	1,455±10	480±3
Medtronic Hall	535±53	4,243±103	1,856±22	745 ±12
Carbomedics	371±16	3,715±101	1,712±8	611±12
ON-X	366±18	4,516±30	1,483±8	147±3

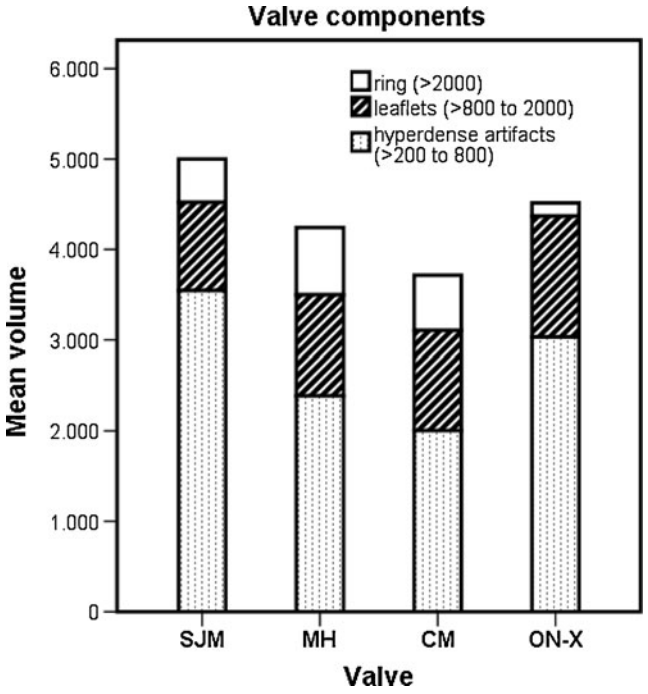

Fig. 3 The mean hyperdense artifact volume (mm^3) in stationary valves differentiated according to leaflet (>800) and prosthetic ring thresholds (>2,000). Significant differences existed between all valves for ring and total artifact volume (*SJM* St Jude; *MH* Medtronic Hall; *CM* Carbomedics)

significant difference was found for the CM valve (p= 0.123), and for SJM and MH valves a mean decrease in hyperdense artifacts was measured for the pulsatile valves (p<0.001 and p=0.018 respectively). Differences were small when compared to the artifact volume (without the radiopaque ring and leaflet components) and were 5%, 6%, and 8% for the ON-X, SJM, and MH valve respectively.

Discussion

This phantom study had the goals to compare various prosthetic heart valves (PHV) with respect to (1) artifacts in stationary valves and (2) artifacts at various phases of the cardiac cycle. To allow for quantification of artifacts, we developed threshold values that allowed for measuring the volumes affected by PHV-induced artifacts. These artifacts can be hypodense or hyperdense relative to their surroundings. We found the least hypodense artifact volumes in stationary CM and ON-X valve and the least hyperdense artifact volumes for stationary CM valves. In a dynamic situation, valve artifacts increased substantially during opening and closing and were least in the closed valve position, independent of the valve type evaluated. In addition, closed pulsatile valves exhibited considerably more hypodense artifacts than closed stationary valves despite very small differences in hyperdense artifacts.

The primary differences in the CT appearance between valves existed in the density of the prosthetic ring. We found the highest ring density in the SJM valve and the lowest in the ON-X valve. These differences are probably due to differences in the components and design of the prosthetic ring. The prosthetic ring consists of the leaflet housing which harbors the hinge points of the leaflets and a rotation mechanism. The rotation mechanism allows rotation of the sewing ring relative to the housing so that the leaflets can be adjusted to the preference of the surgeon. Manufacturers use specific mechanisms to enable rotation. For SJM valves differences exist even between valve types. The first SJM valves were non-rotatable and thus consisted of only radiopaque leaflets. In a clinical series, these valves had excellent visibility of periprosthetic tissues [12]. Rotatable SJM valves ("Master" and "HP" series) have three metal components in the mechanism: two rings and a spring. These components are made of metal alloys containing nickel. The latest SJM type (Regent) has one metal component which is made of a cobalt-nickel alloy. As we have only tested the SJM Master valve, we cannot comment on possible differences in image quality with the SJM Regent type. The MH valve consists of one piece of non-coated titanium alloy (Ti6Al4V) that forms both the housing for the occluder disc and the prosthetic ring to which a sewing cuff is attached. It has more titanium than other valves because of the central struts of the retaining mechanism. The CM valve has a rotation mechanism that is integrated in the leaflet housing with a titanium stiffening ring and a nitinol (a nickel-titanium alloy) locking ring. Finally, the ON-X valve has a rotation mechanism with two thin titanium alloy rings (Ti6Al4V) embedded in the carbon structure of the housing. Despite the seemingly uniform composition with the use of titanium in three of the valves, the differences in the metal volume and other parts of the rotation mechanism may account for the different ring densities.

With respect to the leaflets, the CM and MH leaflets had higher densities than the SJM and ON-X valves. These leaflets consist of a graphite substrate over which pyrolytic carbon is applied. The graphite contains commonly 10% tungsten for the visualization of leaflet motion with fluoroscopy. Except for the ON-X valve, the pyrolytic carbon contains 5–12% silicon for hardness and wear stability. The differences in leaflet density may be explained by differences in the amount of tungsten used. Furthermore, the quite variable densities measured in the leaflets (as reflected by the large SD) may well be explained by the

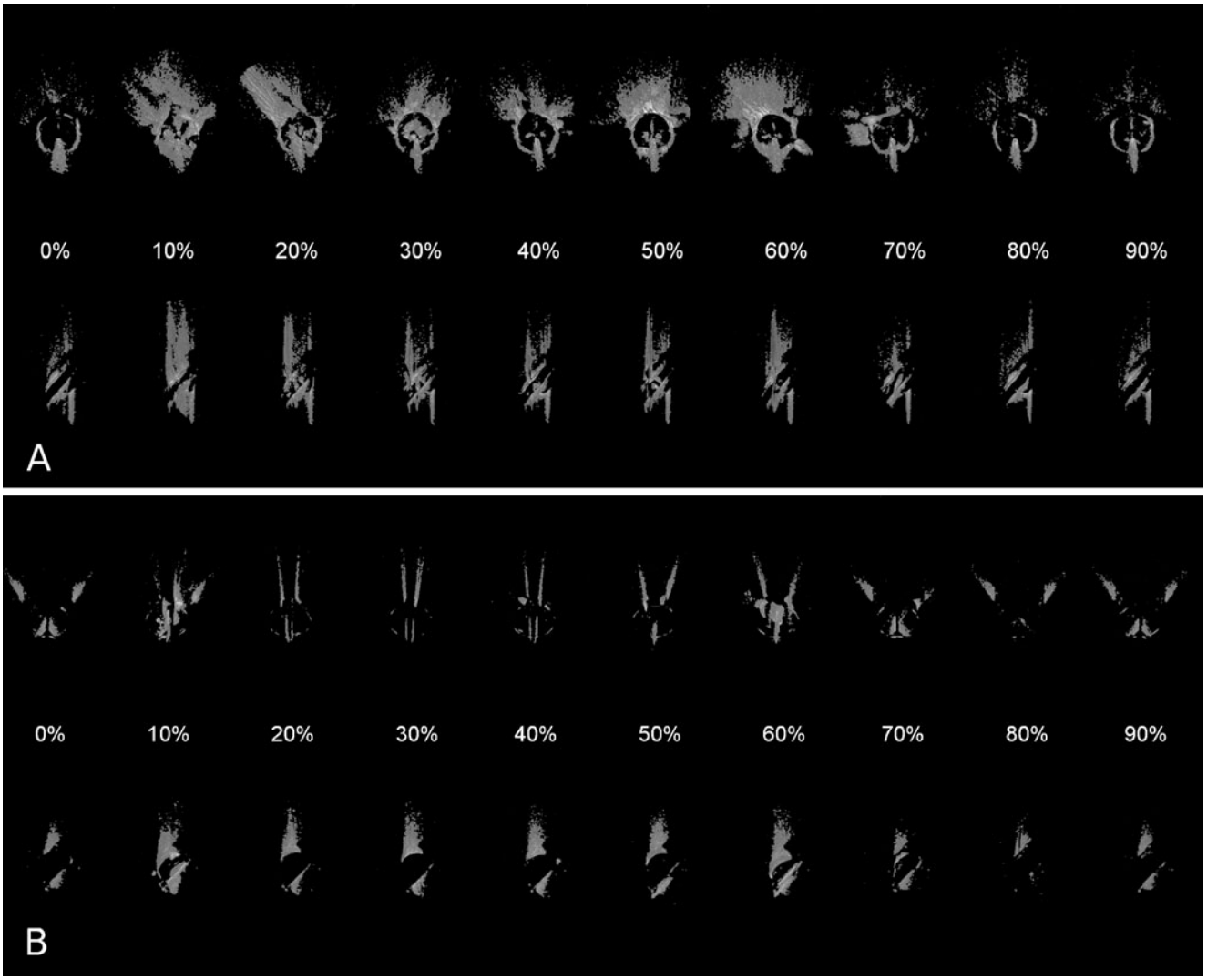

Fig. 4 Volume rendered images of hypodense artifact distribution patterns for the tilting disc Medtronic Hall valve (**a**) and the bileaflet ON-X valve (**b**). In each series, the upper panel represents a frontal view and the lower panel represents a side view of the artifact volumes identified with the −50 HU threshold. Leaflet motion is present in the following ECG intervals: at 10 and 20% (opening) and at 60 and 70% (closing). At 30–50% the valve is opened and from 80 to 90 and 0% the valve is closed

over projection of the artifacts emanating from the prosthetic ring.

The thresholds derived from the surrounding structures approximate the clinically encountered densities of periprosthetic structures which range from −50 to 200 HU. In contrast to the −50 HU threshold which delineates only artifacts, the 200 HU threshold includes all radiopaque parts of a valve. These radiopaque parts were further characterized with the two thresholds derived from the prosthetic leaflets and ring. This differentiation of ring and leaflet volumes from the total hyperdense artifacts measured with the 200 threshold demonstrated the individual differences between the valves. For example, despite a very low ring volume, the ON-X valve had the highest leaflet volume. This could be explained by a steeper closure angle of the ON-X (40°) when compared to the other valves (not more than 25°), therefore necessitating a larger leaflet volume. Also, the SJM valve had the most artifacts (hyper- and hypodense) despite a relatively low leaflet volume and ring volume. Possibly, this may be related to the different ring composition which contains nickel instead of titanium such as the other valves. Furthermore, the highest ring volume of the MH valve is explained by the extensive central strut mechanism which is not present in the other valves. Therefore, all these differences may be related to specific design and composition of the valves.

Earlier reported visual image quality scoring revealed best image quality for the CM and ON-X valves [11, 12].

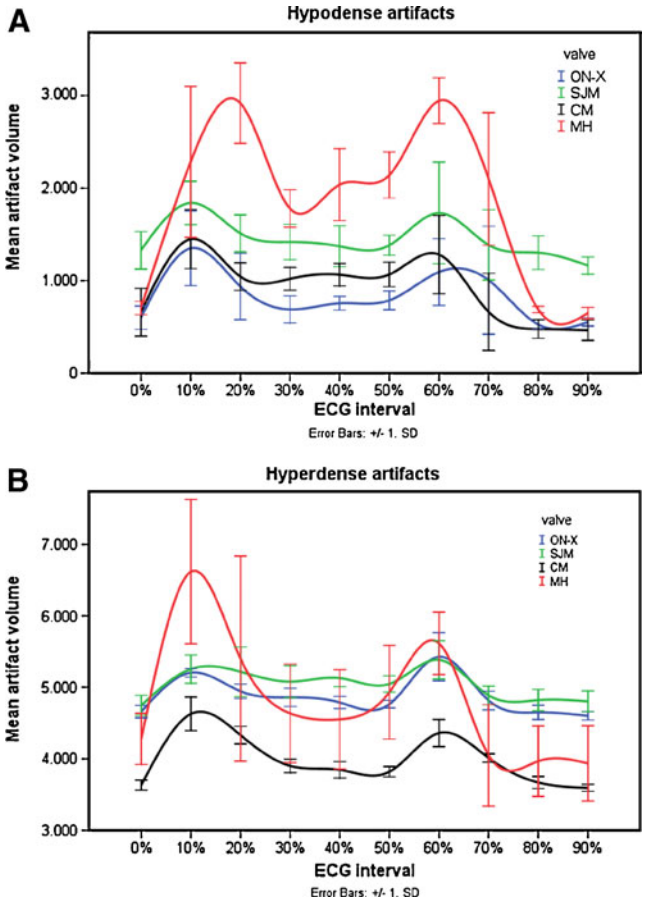

Fig. 5 Graphs show hypodense (**a**) and hyperdense (**b**) artifact volumes measured with the −50 (hypodense) and 200 (hyperdense) thresholds, respectively during the 10 ECG intervals. Leaflets were closed at 0%, opening at 10%, were opened at 30–50% and were closing at 60% of the ECG interval (*SJM* St Jude; *CM* Carbomedics; *MH* Medtronic Hall)

The MH and SJM valves were associated with good albeit lesser image quality. The current results show a similar ranking for the hypodense artifacts. For the hyperdense artifacts, the CM and MH valves are superior to the ON-X valve, which in turn is superior to the SJM valve.

Pulsatile valves showed an important variation in artifacts which was related to the phase of leaflet motion. For both types of artifacts, the closed phase was associated with the least artifacts, followed by the completely opened phase. Rapid leaflet motion increased the artifacts and ideally CT data acquisition during phases with leaflet motion should be avoided. The amount of variation in hypodense artifacts was increased for MH valve when compared to the other valves and could be related to the tilting disc design.

The finding that closed pulsatile valves emanate more hypodense artifacts than closed stationary valves suggests various mechanisms of artifact formation. It is unlikely that physics-based artifacts such as beam hardening and photon starvation account for these differences because these mechanisms would expected to be equally present in both stationary and pulsatile closed valves. Other possible explanations are data discrepancies in multisector reconstructions or helical interpolation algorithms [13]. In the pulsatile model minute oscillating movement of the valve is possible by the reverberations of the water column after the closure of the leaflet. However, motion would result in double contours and thus an increase in hyperdense artifacts. Instead, we found a decrease of hyperdense artifacts in two valves and very small differences overall. Additional experiments are required to confirm our findings and to further elucidate the generation of PHV-related artifacts.

This study has several limitations. First, our experiments were devoid of annular motion. Although the role of leaflet motion as a source of artifacts is evident from our experiments, clinical CT inevitably involves important annular motion which may negatively affect image quality. Annular motion during systole and diastole may occur in concert with rapid leaflet motion and these phases of the cardiac cycle may produce the least diagnostic image due to the increased artifacts. Other limitations of the study relate to the angulation of the valves in the CT gantry and pulsation pattern. The orientation of neurosurgical titanium clips in relation to the CT plane has been shown to influence the amount of artifacts [4]. We compared all valves under a 45° angle to the CT acquisition plane in an attempt to approximate the angulations encountered clinically. Because of the considerable variation in the aortic annular plane, artifacts and consequently image quality may differ between patients. Another limitation is the lack of physiological pressures in our model. Pulsatile motion in our in vitro model was tailored to study the artifacts emanating from the valves and the "systole" exceeded the physiological duration.

For future testing, threshold filters may provide a measure for artifact reduction strategies. Possible artifact reduction strategies could focus on 1) adjustment of exposure parameters, 2) applying metal filters, 3) iterative reconstruction algorithms. The first method found that an increase of kV proved to be simple and effective in the case of neurosurgical clips. Chenot et al. [14] achieved good results for clinical imaging of bioprostheses using a higher kV. This, however, causes an increase in radiation exposure. A reduction of radiation exposure may be achieved with prospectively triggered imaging of key R-R intervals. The latter two methods have recently become available and are currently being explored for PHV imaging.

In summary, our technique allows for quantitative comparison of artifacts from different valve types. Artifacts are primarily affected by the composition and design of the

valve. The CM valve was associated with the least artifacts. Leaflet motion causes increases in artifacts and the best imaging results may be expected at during phases in which the leaflets are closed.

Conflict of interest None.

References

1. Watzke O, Kalender WA (2004) A pragmatic approach to metal artifact reduction in CT: merging of metal artifact reduced images. Eur Radiol 14:849–856
2. Mahnken AH, Raupach R, Wildberger JE, Jung B, Heussen N, Flohr TG, Günther RW, Schaller S (2003) A new algorithm for metal artifact reduction in computed tomography: in vitro and in vivo evaluation after total hip replacement. Invest Radiol 38:769–775
3. Yu L, Li H, Mueller J, Kofler JM, Liu X, Primak AN, Fletcher JG, Guimaraes LS, Macedo T, Mc Collough CH (2009) Metal artifact reduction from reformatted projections for hip prostheses in multislice helical computed tomography: techniques and initial clinical results. Invest Radiol 44:691–696
4. van der Schaaf I, van Leeuwen M, Vlassenbroek A, Velthuis B (2006) Minimizing clip artifacts in multi CT angiography in clipped patients. Am J Neuroradiol 27:60–66
5. Teshima H, Hayashida N, Fukunaga S, Tayama E, Kawara T, Aoyagi S, Uchida M (2004) Usefulness of a multidetector-row computed tomography scanner for detecting pannus formation. Ann Thorac Surg 77:523–526
6. Tsai IC, Lin YK, Chang YFuYC, Wang CC, Hsieh SR, Wei HJ, Tsai HW, Jan SL, Wang KY, Chen MC, Chen CC (2009) Correctness of multi-detector-row computed tomography for diagnosing mechanical prosthetic heart valve disorders using operative findings as a gold standard. Eur Radiol 19:857–867
7. Symersky P, Budde RPJ, de Mol BAJM, Prokop M (2009) Comparison of multidetector-row computed tomography to echocardiography and fluoroscopy for evaluation of patients with mechanical prosthetic valve obstruction. Am J Cardiol 104:1128–1134
8. Konen E, Goitein O, Feinberg MS, Eshet Y, Raanani E, Rimon U, Di-Segni E (2008) The role of ECG-gated MDCT in the evaluation of aortic and mitral mechanical valves: initial experience. Am J Roentgenol 191:26–31
9. Girard SE, Miller FA, Orszulak TA, Mullany CJ, Montgomery S, Edwards WD, Tazelaar HD, Malouf JF, Tajik AJ (2001) Reoperation for prosthetic aortic valve obstruction in the era of echocardiography: trends in diagnostic testing and comparison with surgical findings. J Am Coll Cardiol 37:579–584
10. Faletra F, Constantin C, De Chiara F, Masciocco G, Santambrogio G, Moreo A, Alberti A, Vitali E, Pellegrini A (2000) Incorrect echocardiographic diagnosis in patients with mechanical prosthetic valve dysfunction: correlation with surgical findings. Am J Med 108:531–537
11. Symersky P, Budde RPJ, Prokop M, de Mol BAJM (2011) Multidetector-row computed tomography imaging characteristics of mechanical prosthetic valves. J Heart Valve Dis 20:216–222
12. Habets J, Symersky P, van Herwerden LA, de Mol BAJM, Spijkerboer AM, Mali WPTM, Budde RPJ (2011) Prosthetic heart valve assessment with multidetector-row CT: imaging characteristics of 91 valves in 83 patients. Eur Radiol. doi:10.1007/s00330-011-2068-8
13. Barrett JF, Keat N (2004) Artifacts in CT: recognition and avoidance. Radiographics 24:1679–1691
14. Chenot F, Montant P, Goffinet C, Pasquet A, Vancraeynest D, Coche E, Vanoverschelde JL, Gerber BL (2010) Evaluation of anatomic valve opening and leaflet morphology in aortic valve bioprosthesis by using multidetector CT: comparison with transthoracic echocardiography. Radiology 255:377–385